EPJ Web of Conferences **105**, 01003 (2015)
DOI: 10.1051/epjconf/201510501003

Measuring TeV cosmic rays at the High Altitude Water Cherenkov Observatory

Segev BenZvi[a]

Department of Physics and Astronomy, University of Rochester, Rochester, NY, USA

Abstract. The High-Altitude Water Cherenkov Observatory, or HAWC, is an air shower array designed to observe cosmic rays and gamma rays between 100 GeV and 100 TeV. HAWC, located between the peaks Sierra Negra and Pico de Orizaba in central Mexico, will be completed in the spring of 2015. However, the observatory has been collecting data in a partial configuration since mid-2013. With only part of the final array in data acquisition, HAWC has already accumulated a data set of nearly 100 billion air showers. These events are used to calibrate the detector angular reconstruction using the shadow of the Moon, and to measure the anisotropy in the arrival directions of cosmic rays above 1 TeV. Using data recorded between June 2013 and July 2014, we have observed a significant 10^{-4} anisotropy consisting of three statistically significant "hotspots" in the cosmic ray flux. We will discuss these first results from HAWC and compare them to previous measurements of anisotropy in the northern and southern sky.

1. Introduction

During the past 10 years, an anisotropy in the arrival directions of TeV cosmic rays has been observed by detectors in both the Northern and Southern Hemispheres. In the north, large-scale ($> 60^\circ$) structures have been reported by the Tibet ASγ Collaboration [1], Super-Kamiokande [2], Milagro [3,4], EAS-TOP [5], MINOS [6], and ARGO-YBJ [7]. In the southern hemisphere, large-scale anisotropies have been observed with the IceCube detector from 20 TeV [8,9] to 2 PeV [10]. The anisotropy is dominated by an approximately 10^{-3} dipolar structure, but small-scale components ($< 60^\circ$) with relative intensities of 10^{-4} have also been observed in both the northern and southern sky.

The origin of the anisotropy is unknown, but calculations of cosmic-ray diffusion from nearby Galactic accelerators suggest that a weak dipole or dipole-like feature should be observed in the TeV cosmic-ray flux [11–14]. The small-scale structure may be the product of turbulence in the Galactic magnetic field [15,16]. However, more exotic origin scenarios such as the decay of quark matter in pulsars [17] or the self-annihilation of dark matter [18] have also been suggested. In this proceeding, we discuss new measurements of the anisotropy at the HAWC Observatory.

2. The HAWC observatory

The High Altitude Water Cherenkov Observatory, or HAWC, is a gamma-ray and cosmic-ray air shower detector located 4100 m above sea level next to Pico de Orizaba, Mexico (Fig. 1). HAWC covers approximately 20,000 m^2 and comprises 300 close-packed water Cherenkov detectors (WCDs). Each WCD is a 7.3 m × 5 m light-tight steel tank containing 200 kL of purified water and four hemispherical photomultiplier tubes (PMTs).

The PMTs are used to detect the Cherenkov light produced when air shower particles pass through the water in the tanks. By combining the timing information and spatial pattern of the PMTs triggered by an air shower, the arrival direction of the air shower can be reconstructed. Using simple topological cuts it is also possible to classify the shower as hadronic or electromagnetic in origin, and hence distinguish cosmic rays from gamma rays.

While construction of the HAWC array is almost complete, the detector has operated in several configurations since regular data taking began in June 2013. In this work we report on data collected with the 95-tank and 111-tank configurations of the detector (henceforth called HAWC-95 and HAWC-111) which operated between June 2013 and July 2014.

3. Anisotropy of cosmic rays

3.1. Data set and quality cuts

During the operation of HAWC-95 and HAWC-111, the detector recorded air showers at a rate of about 15 to 20 kHz. Between 12 June 2013 and 8 July 2014, HAWC operated with a total livetime of 4332.1 hours, or about 181 days, recording 8.6×10^{10} events during this period.

To select events suitable for an anisotropy analysis, we applied the following selection criteria:

- Only data from full data acquisition runs (contiguous 24-hour periods of observation) are used;

[a] e-mail: sybenzvi@pas.rochester.edu

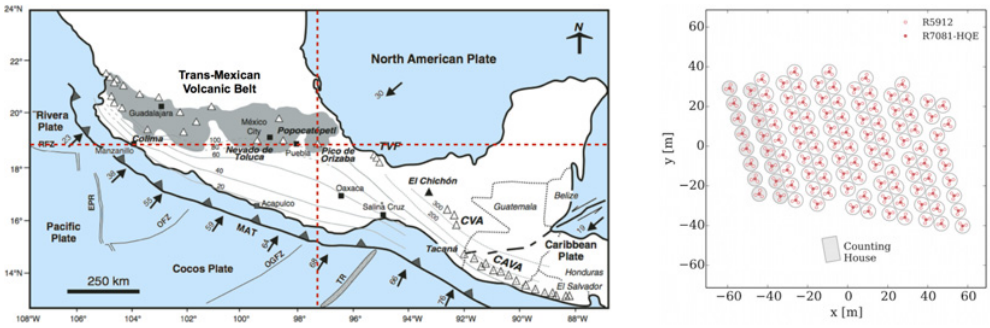

Figure 1. *Left*: location of HAWC site, indicated by dashed cross (map from [19]). *Right*: configuration of the water Cherenkov detectors and PMTs for the data set described in this work. The 95-tank configuration of HAWC (HAWC-95) is shown in white; the additional two rows of tanks added to make the 111-tank configuration of HAWC (HAWC-111) are shown in gray.

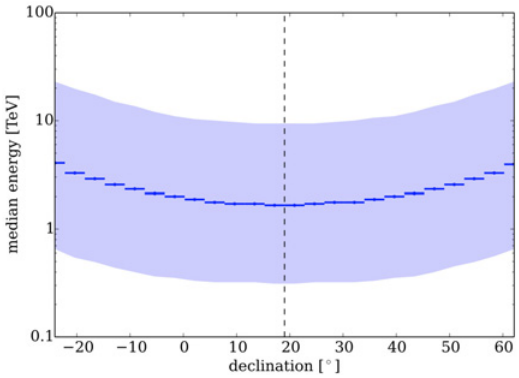

Figure 2. Median energy of the cosmic-ray data set used in this analysis, plotted as a function of declination. The light blue contour indicates the central 68% of the energy distribution, and the dashed line indicates the zenith above the HAWC detector, which is located at 19°N latitude.

- The core and angle fit of the air shower must be successful;
- The number of PMTs triggered by the event must be ≥ 30.

Approximately 113 days of data, corresponding to 4.9×10^{10} events, survive the quality cuts. Using air shower and detector simulations based on the CORSIKA and GEANT4 codes [20,21], we estimate that the resulting sample of air showers has a median energy of 2 TeV and a median angular resolution of 1.2°. As shown in Fig. 2, the median energy increases with shower zenith; this is a trigger threshold effect caused by the increase in atmospheric overburden at large zenith angles.

We note that the data set includes gamma rays because no criterion was applied to remove electromagnetic showers. However, the contamination produced by gamma rays is effectively negligible, since the gamma-ray flux from even the most intense point sources is <0.1% of the cosmic-ray flux.

3.2. Analysis technique

To measure the anisotropy of cosmic rays observed by HAWC, the quantity of interest is the relative intensity of the cosmic rays, defined as the integral flux in a finely binned sky map:

$$\delta I(\alpha_i, \delta_i) = \frac{\Delta N_i}{\langle N \rangle_i} = \frac{N(\alpha_i, \delta_i) - \langle N(\alpha_i, \delta_i) \rangle}{\langle N(\alpha_i, \delta_i) \rangle}. \quad (1)$$

In this expression, $N(\alpha_i, \delta_i)$ corresponds to the number of air showers recorded from the i^{th} bin with celestial coordinates (α_i, δ_i). The relative intensity expresses the difference between the observed and expected counts $\langle N \rangle_i$, where the expected counts in each bin are estimated using the data themselves [22,23]. Sky maps of relative intensity as a function of celestial coordinates can be rebinned to enhance the appearance of significant regions of excess or deficit flux. The statistical significance of excesses and deficits is reported in terms of Gaussian σ using the method of Li and Ma [24].

It is also possible to perform a Legendre decomposition of the relative intensity,

$$\delta I(\alpha_i, \delta_i) = \sum_{\ell=0}^{\infty} \sum_{m=-\ell}^{\ell} a_{\ell m} Y_{\ell m}(\pi - \delta_i, \alpha_i) \quad (2)$$

which we use to produce an angular power spectrum

$$C_\ell = \frac{1}{2\ell + 1} \sum_{m=-\ell}^{\ell} |a_{\ell m}|^2. \quad (3)$$

3.3. Verification: Observation of the moon shadow

To verify the reconstruction of cosmic-ray showers and study the energy of the data set, we can observe the deficit of cosmic rays, or "shadow," produced by by the absorption of cosmic rays in the lunar surface. The Moon shadow is shown in Fig. 3 in terms of relative intensity δI and significance. In the HAWC-95 and HAWC-111 data we observe a deep deficit produced when the Moon transits across the sky. The deficit accumulates at the rate of about $2.4\sigma/\sqrt{\text{transit}}$.

In lunar-centric sky coordinates, the deficit is offset from the true position of the Moon by $\Delta\alpha = 0.91° \pm 0.04°$. The offset is produced by the deflection of cosmic

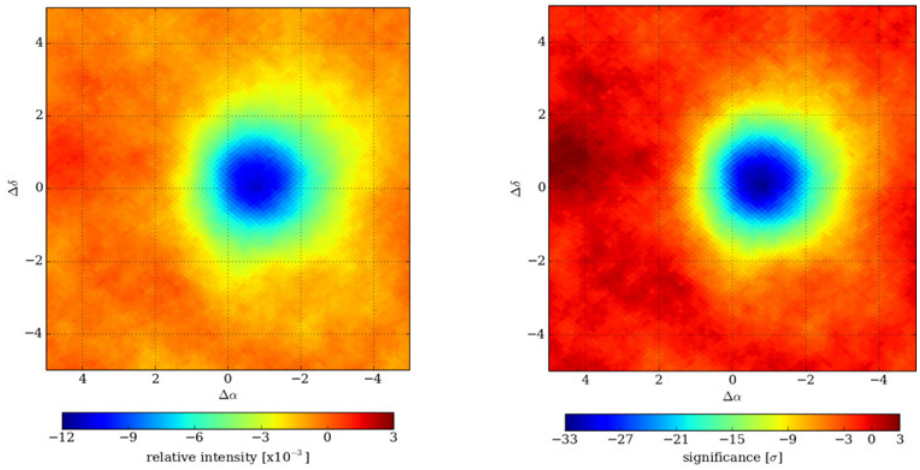

Figure 3. Shadow of the Moon in cosmic rays, shown in terms of relative intensity (left) and Li-Ma significance (right).

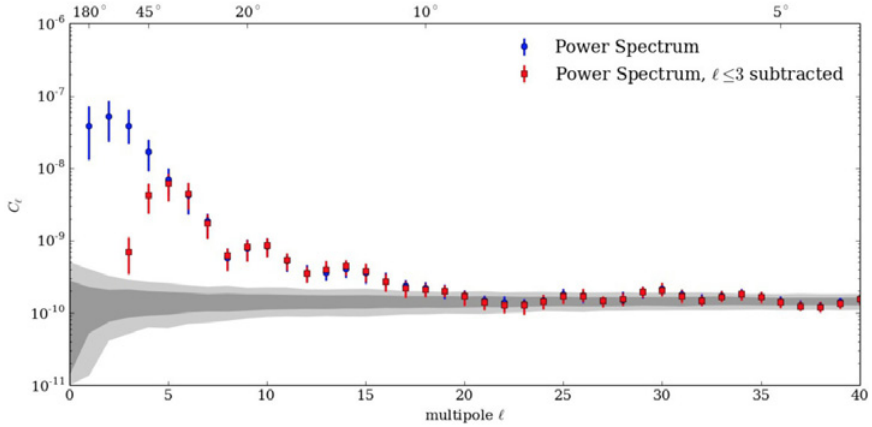

Figure 4. Angular power spectrum of the relative intensity of cosmic rays observed with HAWC-95 and HAWC-111. The full power spectrum, corrected for the partial-sky coverage of the array, is plotted using blue circles. The power spectrum after the subtraction of the four lowest multipoles of the distribution (via a fit to the large-scale structure) is plotted using red squares.

rays in the geomagnetic field, an effect that is expected to be approximately $\delta\alpha \approx 1.6^\circ \cdot Z(E/\mathrm{TeV})^{-1}$ for cosmic rays of charge Z and energy E [25]. Hence, the observed offset of the Moon shadow is consistent with the mean energy of the data set inferred from simulations (∼2 TeV), and its position verifies the accuracy of the absolute pointing of the detector reconstruction.

3.4. Anisotropy: Sky map and power spectrum

We have carried out an analysis of anisotropy in the 113 days of high-quality data from the HAWC-95 and HAWC-111 detectors. After estimating the expected counts $\langle N(\alpha_i, \delta_i)\rangle$ in each location in the sky, we calculate the relative intensity δI and apply the Legendre decomposition described in Eq. (2). From this we produce the angular power spectrum shown in Fig. 4. The power spectrum indicates the presence of structure at both large ($\ell < 5$) and small ($\ell > 5$) angular scales. This structure is not an effect of partial sky coverage, which we correct for in the analysis.

While the large scale structure in the arrival directions of cosmic rays provides significant power, the HAWC data are distorted because the data set does not cover a full year. As a result, the large-scale structure is contaminated by the "solar dipole," an anisotropy produced by the motion of the Earth around the sun (see [23] for details).

Rather than attempt to correct for the solar dipole effect with only a partial year of data, we elected to fit the lowest 4 terms of Eq. (2) (DC offset, dipole, quadrupole, and octupole) to the data and subtract the fit from the relative intensity δI. The resulting residual power spectrum is shown in Fig. 4, and the residual sky map is plotted in Fig. 5.

After the subtraction of the largest features in the sky map, three regions of excess flux are observed with post-trials significance $>5\sigma$. The first, called Region A, is centered near $\alpha = 60^\circ$. This region coincides with a similar spectrally hard excess observed by the Milagro Collaboration [3] and ARGO-YBJ [7]. This region does not appear in the sky map produced by IceCube [9], though we note that the median energy of the IceCube data is substantially higher (about 20 TeV). The second region of excess flux, labeled Region B, is observed in the ARGO data and also appears to connected to a similar feature in the southern sky observed (at much higher energy) by

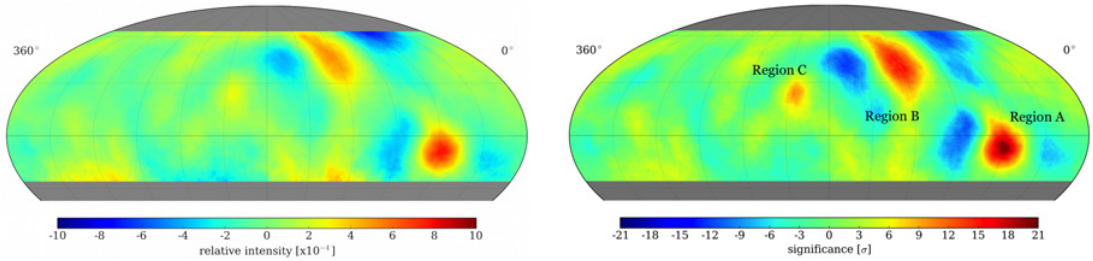

Figure 5. *Left*: relative intensity δI of cosmic rays observed by HAWC-95 and HAWC-111, plotted in celestial coordinates. Large scale structures in the map have been subtracted out (see text for discussion). *Right*: significance of features in the residual sky map. Three excess regions marked A, B, and C are significant at $>5\sigma$ after statistical trials are taken into account.

the IceCube Collaboration. Finally, Region C, located at a right ascension of 210°, appears to confirm a similar excess reported by ARGO-YBJ.

We note that in the discussion of excess counts, the regions with deficits should not be neglected. If the small-scale structure observed in the data is caused by distortions of the large-scale "dipole" anisotropy in turbulent magnetic fields, then the deficits are also physically significant. However, in the HAWC-95+111 data set, none of the observed deficits have significance $> 5\sigma$ after accounting for statistical trials. We will report on the significance of excess and deficit regions with future data.

4. Conclusion

As of this writing, the full configuration of HAWC is now in data acquisition. Cosmic ray air showers will continue to be observed with an event rate $>$ 20 kHz. In the current data set, the small-scale structures observed in the Northern Hemisphere appear to match previous measurements made by the Milagro, ARGO-YBJ, and Tibet ASγ Collaborations. Future results will include measurements of the large-scale anisotropy, corrected for systematic effects such as partial-sky coverage and partial-year observations.

References

[1] M. Amenomori et al. (Tibet ASγ), Astrophys. J. **626**, L29 (2005)
[2] G. Guillian et al. (Super-kamiokande), Phys. Rev. D **75**, 062003 (2007)
[3] A.A. Abdo et al. Phys. Rev. Lett. **101**, 221101 (2008)
[4] A.A. Abdo et al. Astrophys. J. **698**, 2121 (2009)
[5] M. Aglietta et al. (EAS-TOP), Astrophys. J. Lett. **692**, L130 (2009)
[6] J. de Jong (MINOS), *Observations of Large Scale Sidereal Anisotropy in 1 and 11 TeV cosmic rays from the MINOS experiment*, in *Proc. 32nd ICRC*, (Beijing, China, 2011)
[7] B. Bartoli et al. (ARGO-YBJ), Phys. Rev. **D88**, 082001 (2013)
[8] R. Abbasi et al. (The IceCube), Astrophys. J. **718**, L194 (2010)
[9] R. Abbasi et al. (IceCube) Astrophys. J. **740**, 16 (2011)
[10] M. Aartsen et al. (IceCube) Astrophys. J. **765**, 55 (2013)
[11] A.D. Erlykin, A. Wolfendale, Astropart. Phys. **25**, 183 (2006)
[12] P. Blasi, E. Amato. JCAP **1201**, 011 (2012)
[13] M. Pohl, D. Eichler. Astrophys. J. **766**, 4 (2013)
[14] L. Sveshnikova, O. Strelnikova, V. Ptuskin. Astropart. Phys. **50-52**, 33 (2013)
[15] G. Giacinti, G. Sigl. Phys. Rev. Lett. **109**, 071101 (2012)
[16] M. Ahlers, Phys. Rev. Lett. **112**, 021101 (2014)
[17] M.A. Perez-Garcia, K. Kotera, J. Silk. Nucl. Instrum. Meth. **A742**, 237 (2014)
[18] J.P. Harding, `arXiv:1307.6537` (2013)
[19] J. Macías, GSA Special Papers **422**, 183 (2007)
[20] D. Heck, G. Schatz, T. Thouw, J. Knapp, J. Capdevielle, Tech. Rep. FZKA-6019 (1998)
[21] S. Agostinelli et al. (GEANT4), NIM **A506**, 250 (2003)
[22] R.W. Atkins et al. (Milagro) Astrophys. J. **595**, 803 (2003)
[23] A.U. Abeysekara et al. (HAWC) Astrophys. J. **796**, 108 (2014)
[24] T.P. Li, Y.Q. Ma, Astrophys. J. **272**, 317 (1983)
[25] S. BenZvi (HAWC), *An All-Sky Simulation of the Response of HAWC to Sources of Cosmic Rays and Gamma Rays*, in Proc. 33rd ICRC (Rio de Janeiro, Brazil, 2013)